1 November 1999

Optics Communications

Optics Communications 170 (1999) 207–212

www.elsevier.com/locate/optcom

Talbot imaging with increased spatial frequency: a technique for replicating truncated self-imaging objects

Wei-Hung Yeh *, M. Mansuripur, M. Fallahi, R. Scott Penner

Optical Sciences Center, University of Arizona, Tucson, AZ 85721, USA

Received 28 October 1998; received in revised form 13 August 1999; accepted 16 August 1999

Abstract

The Talbot effect in the presence of a convergent beam of coherent light yields a demagnified image of a self-imaging object. In fact, the object does not even have to fulfill the self-imaging condition; the object with truncated self-imaging feature is sufficient to yield an image that is sufficiently accurate for many practical purposes. We have taken this approach to fabricating circular gratings with a reduced period compared to the period of the mask. Using a simple experimental setup and a concentric circular grating mask, we have created images whose periods are either one-half or one-third of the mask's period. Demagnified Talbot imaging of fully or truncated self-imaging objects provides an attractive approach to photolithographic fabrication of structures whose periods are somewhat greater than the wavelength of the light source.

1. Introduction

The well-known Talbot effect [1–4] is a useful tool in diverse applications [5–8]. For those objects satisfying the condition of self-image formation [3,9,10], the Talbot effect provides an efficient method for duplicating self images or multiple images of the object with plane wave illumination, or for generating magnified images of the object with spherical wave illumination.

These self-imaging objects may show laterally-periodic or radially-periodic structure. Although a circular grating is not strictly a Talbot object (instead it is a truncated self-imaging object) [10,11], it may be shown that its radially periodic nature is sufficient to produce self images over most of the grating's area.

In the presence of a convergent beam, the Talbot effect can increase the spatial frequency of these objects. In contrast to the case of fractional Talbot effect where the increased spatial frequency arises from the creation of multiple shifted images [8,12], the increased frequency obtained with a convergent beam is solely due to image demagnification. Based on the theories of diffraction and geometrical optics [2,4,13], the increased spatial frequency of the demagnified Talbot image can be of the order of the wavelength of the light used for illumination. This makes it an attractive method for optical lithography and mass-production of photonic and electronic com-

* Corresponding author. Tel: +1-510-353-9700x258; fax: +1-510-353-1845; e-mail: wyeh@maxoptix.com

0030-4018/99/$ - see front matter
PII: S0030-4018(99)00456-3

ponents with submicron periodic (or radially-periodic) structures. Examples of such structures include circular gratings used in certain types of lasers [14], circular or spiral grooves of an optical disk, and dynamic random-access memory (D-RAM) chips.

In this paper we describe the experimental results pertaining to the fabrication of the Talbot image with increasing spatial frequency by using a convergent beam and a circular grating. A concentric circular grating is used as a mask, and its demagnified Talbot image is formed on a photoresist layer. The fabricated grating's spatial frequency is several times greater than that of the mask.

2. Experimental setup and results

The setup for recording a reduced Talbot image is shown in Fig. 1. The light source is an argon ion laser operating at $\lambda = 488$ nm. To reduce the effect of spherical aberrations due to the thickness of the mask, an objective lens with small NA ($= 0.25$) was chosen. The masks used were concentric circular gratings having different periodicities. Although both amplitude and phase gratings should work in this scheme, amplitude gratings were chosen because of the high contrast ratio obtained at the image plane. The masks were fabricated by coating a glass substrate with a 100 nm-thick layer of aluminum. Concentric circular gratings were then defined by electron beam lithography into PMMA resist. After development, the patterns were transferred into the mask by electron cyclotron resonance reactive ion etching (ECR-RIE) of the aluminum layer in a Cl_2:He mixture.

Two sets of circular gratings were fabricated on the mask: one with a pitch of 5 μm (2 μm lines, 3 μm spaces) and a total radius of 375 μm, another with a period of 2 μm (0.8 μm lines, 1.2 μm spaces) and a total radius of 500 μm. Fig. 2 shows photomicrographs of these masks.

Photographs of the light intensity distribution at the focal plane of the objective lens are shown in Fig. 3, revealing the Fourier components of the gratings. Both pictures show the dominance of the zeroth and the first order diffracted beams. The apparent splitting or fine-structure of the first order rings is mainly due to the fact that circular grating is not strictly composed from Bessel functions, to which discrete circular diffraction orders correspond.

A photoresist-coated glass substrate was used to record the reduced Talbot image of the grating. To correct the longitudinal misalignment and adjust the position of the recording plate, the imaging system shown behind the recording plate in Fig. 1 was used to monitor the image at the photoresist layer. The distance between the mask and the recording plane is 1060 ± 5 μm for Sample 1 (i.e., the grating with a

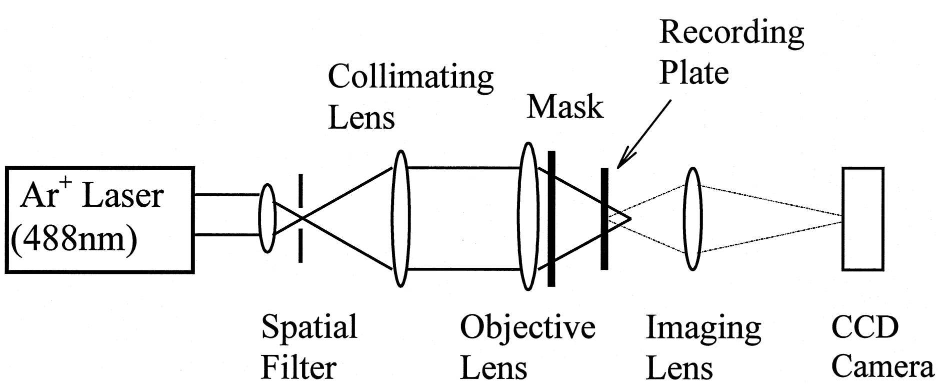

Fig. 1. Diagram of the experimental setup for forming the reduced Talbot image on a photographic plate. The microscope objective lens (NA = 0.25) produces the convergent beam that illuminates the mask. The mask is immediately behind the objective lens, and the recording plate is placed between the mask and the focal plane of the lens. To correct the longitudinal misalignment, the imaging system behind the recording plate is used to monitor the position of the Talbot image relative to the photoresist layer.

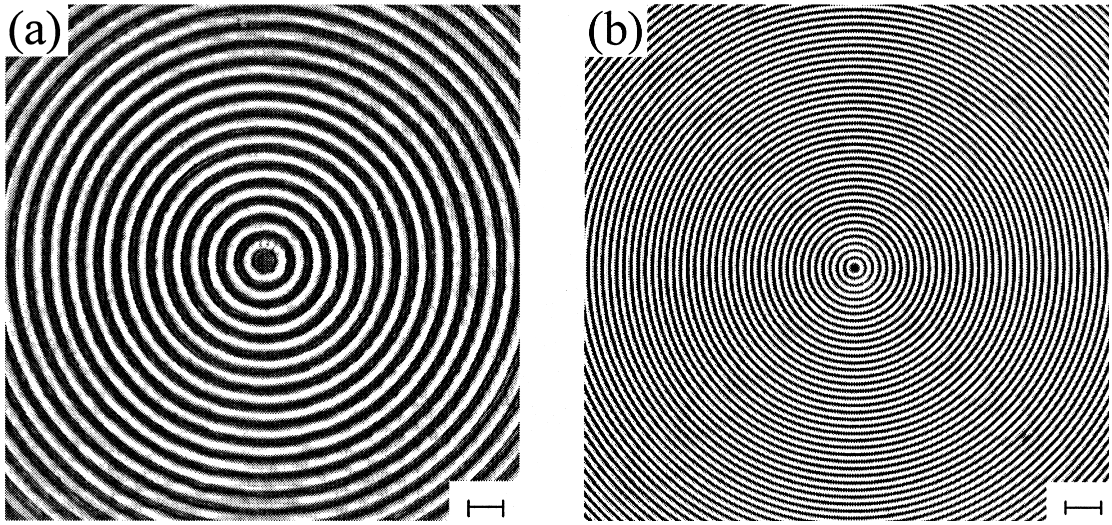

Fig. 2. Photomicrographs of circular gratings used as masks. (a) grating with a period of 5 μm and a total radius of 375 μm; (b) grating with a period of 2 μm and a total radius of 500 μm. The scale bar on the graphs corresponds to 10 μm in both cases.

period of 5 μm), and 835 ± 5 μm for Sample 2 (i.e., the grating with a period of 2 μm). The distance between the recording plane and the focal plane of the lens is 420 ± 5 μm for the first sample and 1070 ± 5 μm for the second sample.

After developing the exposed sample, we inspected the patterns under a scanning electron microscope (SEM). Fig. 4 shows the SEM micrographs of the 1.4 μm-period grating obtained from Sample 1, namely, the 5 μm-period mask, corresponding to a

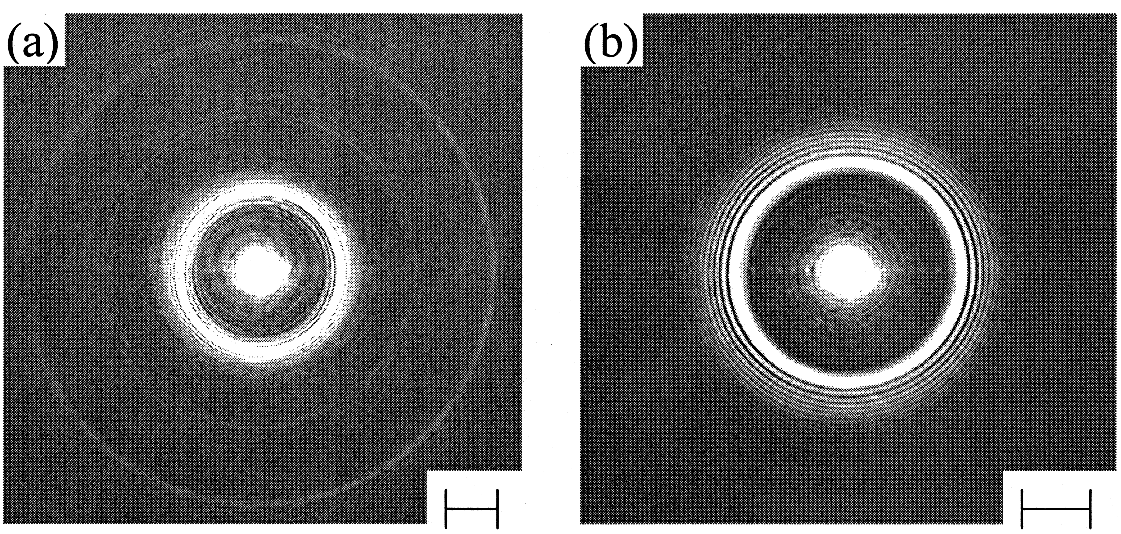

Fig. 3. Photograph showing the Fourier spectrum in the focal plane of the objective lens when a circular grating mask is placed immediately after the lens. (a) 5 μm-pitch grating: the scale bar on the graph is 100 μm-long; (b) 2 μm-pitch grating: the scale bar is 300 μm-long.

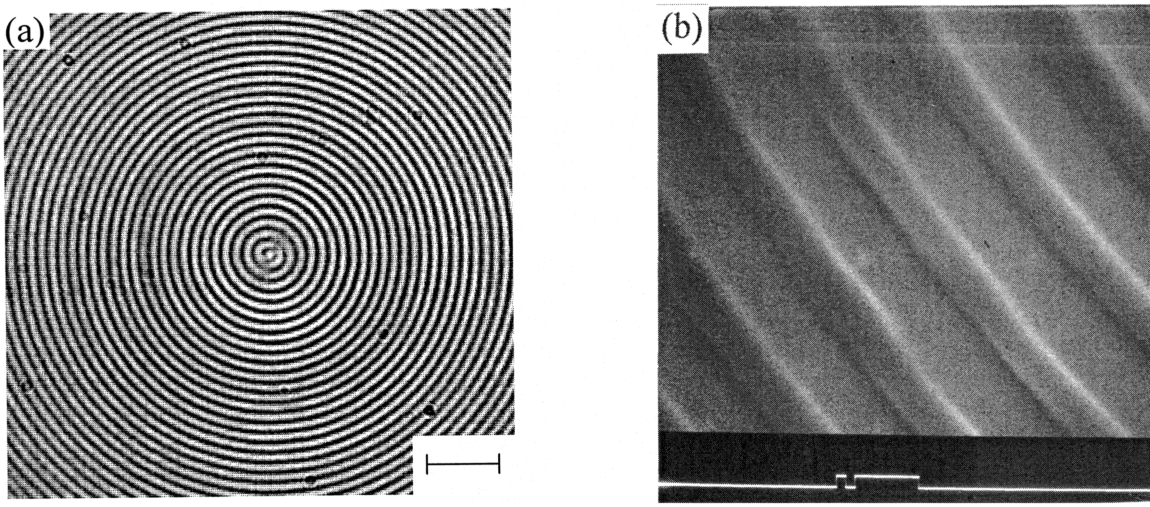

Fig. 4. (a) Photomicrograph of the recorded Talbot image of Sample 1. The original 5 μm-period of the grating has been reduced to 1.4 μm. The scale bar on the graph is 10 μm-long. (b) SEM micrograph showing the detailed structure of some of the lines. The scale bar on the graph is 1 μm-long.

demagnification factor of 3.6. Using the second mask (i.e., the 2 μm-period circular grating), a 1.1 μm-period grating was obtained with a demagnification factor of 1.8, as shown in Fig. 5. The central region of this grating had been overexposed due to a concentration of optical energy from nearby rings and the outmost region had been underexposed due to the walk-off of optical energy. Because of the hard-clipping response of the photoresist used for the recording material, the resulted binary patterns may be optimized by choosing different exposure and develop time. Besides those regions, which fortunately are not used in the format of the optical disk, all the other rings appeared to be well defined.

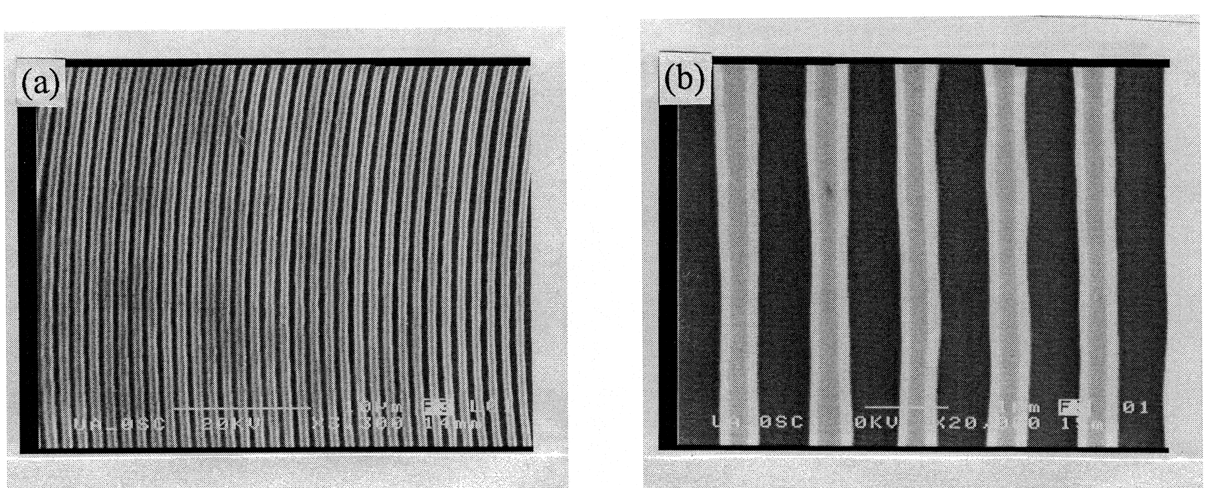

Fig. 5. SEM micrographs of the recorded Talbot image of Sample 2. The original 2 μm-period of the grating has been reduced to 1.1 μm. The high-magnification image in (b) shows the detailed structure of some of the lines.

3. Discussion

By using a deep UV light source in conjunction with an optimized Talbot setup, it should be possible to produce gratings with periods below 0.5 μm from a mask with a period in the range of 1–2 μm. This might provide an alternative fabrication technique for the production of unconventional locally periodic structures, such as spiral or circular gratings. In our experiments (conducted at $\lambda = 488$ nm) we noticed certain features of the demagnified Talbot image that are perhaps worth mentioning at this point.

3.1. Phase reversal

The nonparabolic approximation of spherical wavefronts obtained by including higher-order terms in the diffraction integrals reveals that due to aberrations the contrast is not uniform over the area of the Talbot image [15,16]. Tilt of the recording plate relative to the optical axis also causes local contrast reversal which could be corrected by using the imaging system shown in Fig. 1. This contrast variation may cause a π phase-shift across the reproduced grating, which will degrade the quality of the final grating at certain locations. Another reason for the decreasing contrast along the radial direction is due to the fact that a circular grating is not strictly a self-imaging object [10].

3.2. Non-uniformity of the duty cycle

Variation of the contrast ratio has another impact on the reduced Talbot image: it results in the variation as a function of radius of the duty cycle of the gratings at the photoresist layer. The light source's Gaussian intensity distribution also causes a variation of the duty cycle over the interference area. A slight variation of the duty cycle may be seen in Figs. 4 and 5. The variation of the line profile on the photoresist layer may be overcome by using a small-NA lens, neglecting those regions of the reproduced grating that are far away from the center, and using a more uniform incident beam.

3.3. Choice of the mask

Based on our experimental findings, it is clear that both masks used in our studies can achieve the same reduced period in the image plane. However, the total number of grooves obtained on the recording plate will be different for each mask. The choice of the mask, therefore, is not only dependent on the manufacturing process (the mask with larger period is easier to fabricate), but also on the desired number of grooves (the mask with smaller period yields more grooves at the end).

4. Concluding remarks

By using the Talbot effect in a convergent beam we obtained a demagnified truncated self-image of a radially-periodic amplitude mask. Gratings with 2–3 fold reduction in their period were successfully printed in photoresist. This technique offers an attractive alternative for large-volume fabrication of sub-micron globally-periodic as well as radially-periodic patterns with enhanced spatial frequencies.

References

[1] F. Talbot, Facts relating to optical science IV, Philos. Mag. 9 (1836) 401–407.
[2] L. Rayleigh, On copying diffraction-gratings, and on some phenomenon connected therewith, Philos. Mag. 11 (1881) 196–205.
[3] W.D. Montgomery, Self-imaging objects of infinite aperture, J. Opt. Soc. Am. 57 (1967) 772–778.
[4] K. Patorski, The self imaging phenomenon and its applications, in: E. Wolf (Ed.), Progress in Optics XXVII, North Holland, Amsterdam, 1989, pp. 1–108.
[5] A.W. Lohmann, D.E. Silva, An interferometer based on the Talbot effect, Opt. Commun. 2 (1971) 413–415.
[6] B. Packross, R. Eschbach, O. Bryngdahl, Image synthesis using self imaging, Opt. Commun. 56 (1986) 394–398.
[7] A.W. Lohmann, J.A. Thomas, Making an array illumination based on the Talbot effect, Appl. Opt. 29 (1990) 4337–4340.
[8] D.C. Flanders, A.M. Hawryluk, H.I. Smith, Spatial period division—A new technique for exposing submicrometer-linewidth periodic and quasiperiodic patterns, J. Vac. Sci. Technol. 16 (6) (1979) 1949–1952.
[9] A.W. Lohmann, J. Ojeda-Castañeda, N. Streibl, Spatial periodicities in coherent and partially coherent fields, Optica Acta 30 (1983) 1259–1266.
[10] D.E. Silva, Talbot interferometer for radial and lateral derivatives, Appl. Opt. 11 (1972) 2613–2624.
[11] P. Szwaykowski, Self-imaging in polar coordinates, J. Opt. Soc. Am. A 5 (1988) 185–191.
[12] J.T. Winthrop, C.R. Worthington, Theory of Fresnel images.

I. Plane periodic objects in monochromatic light, J. Opt. Soc. Am. 55 (1965) 373–381.
[13] P. Latimer, Talbot plane patterns: grating images or interference effects?, Appl. Opt. 32 (1993) 1078–1083.
[14] M. Fallahi, F. Chatenoud, M. Dion, I. Templeton, R. Barber, J. Thompson, Circular-grating surface emitting distributed Bragg reflector lasers on an InGaAs-GaAs structure for 0.98-μm applications, IEEE J. Sel. Topics Quantum Electron. 1 (2) (1995) 382–386.
[15] Y. Cohen-Sabban, D. Joyeux, Aberration-free nonparaxial self-imaging, J. Opt. Soc. Am. 73 (1983) 707–719.
[16] K. Patorski, S. Kozak, Self-imaging with nonparabolic approximation of spherical wavefronts, J. Opt. Soc. Am. A 5 (1988) 1322–1327.